Dual-Connectivity Prevenient Handover Scheme in Control/User-Plane Split Networks

Ping-Jung Hsieh, Wei-Shih Lin, Kuang-Hsun Lin, and Hung-Yu Wei

***Abstract*—A control/user (C/U) plane-split network, where macro- and microevolved Node Bs (eNBs) are responsible for C/U-planes, respectively, is a potential 5G solution to address the problems experienced by high-speed railway communication systems such as frequent handovers (HOs), low system capacity, and low data rate. The C-plane transition occurs during an intermacro eNB HO to reduce the frequency of HOs. However, the intermacro-eNB HO in a C/U-plane-split network is prone to handover failures (HOFs) and long service interruption time similar to the traditional long-term evolution-advanced (LTE-A) HO without improvements because it is similar to an LTE-A HO between macro-eNBs from the perspective of C-plane transition. In this paper, we realize a C/U-plane-split network using the LTE-A dual-connectivity (DC) technique and propose a dc-based prevenient HO (PHO) scheme to improve the robustness of the intermacro-eNB HO. The proposed scheme specifically is an *a priori* method and uses the transmit diversity based on the dc technique to reduce the risk of HOFs and the long service interruption time. Further, we first develop the analytical expressions for HO performance for PHO and LTE-A HO, where HOFs are aligned with the LTE-A specifications such that they are defined as the association between the radio link monitor and HO processes. The analytical results are verified against simulation results. Through simulations, we compare PHO with LTE-A HO and the representative schemes of the previous literature in a variety of mobility performance metrics (such as the averages of the successful HO rate, the HOF rate, the radio link failure rate, the ping-pong rate, and the service interrupt time). The results confirm that the proposed scheme achieves superior performance in the key metrics of the successful HO rate and service interrupt time.**

***Index Terms*—Control/user (C/U) plane split, dual connectivity, fifth generation (5G), handover, high-speed railway, radio link failure, radio link monitor.**

I. Introduction

TODAY, high-speed rail is one of the most popular transportation systems in many countries. In addition to fast travel, train passengers on board can enjoy mobile broadband service using their mobile devices. For mobile communication, a current and mature solution is 3rd Generation Partnership Project (3GPP) Long Term Evolution-Advanced (LTE-A) [1]. To provide effective quality of service (QoS) to the User Equipment (UE) on board, LTE study items regarding high-speed rail scenarios have been proposed. In [2], [3], adopting mobile relays (MRs) reduces the signalling load caused by the large number of handover (HO) procedures triggered by the UEs in the same carriage at the same time. Further, adopting a heterogeneous network (HetNet), which combines macro evolved Node Bs (eNBs) with micro/small eNBs, provides an acceptable space diversity gain to enhance the system capacity for the UEs [4]. However, in a HetNet, frequent HOs (between the macro and micro/small eNBs or between the micro/small eNBs) remain a challenge because the cell density is high. Each HO requires a control plane (C-plane) transition and a user plane (U-plane) transition from the serving eNB to the target eNB. The C/U-planes are responsible for the control signaling and the data handling respectively. Consequently, the C-plane signalling load and the occurrences of U-plane transmission interruptions increase significantly because of the frequent HOs in the HetNet.

To address the problems in an HetNet, a 5G potential solution, C/U-plane-split architecture, was proposed in [5], [6]. The split C/U-plane means that a macro eNB is responsible for the C-plane (and also U-plane) with low frequency bands, and the micro/small eNBs manage only the U-plane with high frequency bands. Thus, when a UE moves among the micro/small eNBs covered by a macro eNB, the UE maintains the same C-plane with the macro eNB. Some C-plane procedures (e.g., radio resource control (RRC) procedures) related to the mobility and connectivity within the micro/small eNBs covered by the macro eNB can be bypassed and replaced by L1/L2 signalling. That is, U-plane transitions among micro/small eNBs do not involve C-plane signalling. That provides the advantage of C-plane signaling savings in C/U-plane-split networks [7]. Different from the high-speed rail scenario, several researches [8], [9] focusing on micro/small eNB deployments scenarios, for example, ultra-dense networks (UDNs) have demonstrated the advantage of the C/U-plane-split architecture through system level simulations.

To achieve a C/U-plane-split HO in a high-speed railway, the authors redesigned the LTE-A HO procedure to adapt it to the C/U-plane-split architecture [10]. Their proposed HO scheme includes two types of HO: intra-macro eNB HO and inter-macro eNB HO. The designs of both HOs are practical and straightforward. However, the inter-macro eNB HO procedure

Manuscript received June 14, 2017; revised October 1, 2017; accepted November 1, 2017. Date of publication November 28, 2017; date of current version April 16, 2018. The work of H.-Y. Wei was supported by Ministry of Science and Technology of Taiwan under Grant MOST103-2221-E-002-086-MY3, Grant MOST104-2622-8-002-002, and Grant MOST105-2221-E-002-014-MY3, and in part by National Taiwan University. The review of this paper was coordinated by Abbas Jamalipour. *(Corresponding author: Hung-Yu Wei.)*

P.-J. Hsieh is with the Department of Electrical Engineering, National Taiwan University, Taipei 10617, Taiwan (e-mail: d00921029@ntu.edu.tw).

W.-S. Lin and K.-H. Lin are with the Graduate Institute of Communications Engineering, National Taiwan University, Taipei 10617, Taiwan (e-mail: frank101417@gmail.com; f03942140@ntu.edu.tw).

H.-Y. Wei is with the Department of Electrical Engineering and Graduate Institute of Communications Engineering, National Taiwan University, Taipei 10617, Taiwan (e-mail: hywei@ntu.edu.tw).

Color versions of one or more of the figures in this paper are available online at http://ieeexplore.ieee.org.

Digital Object Identifier 10.1109/TVT.2017.2778065

is inefficient because it includes two sequential HOs: the macro-macro HO (i.e., the HO between the serving and target macro eNBs) for C-plane transition and the phantom-phantom HO (i.e. the HO between the serving and target micro eNBs) for U-plane transition. Both the macro-macro and phantom-phantom HO conditions must be achieved for a successful inter-macro eNB HO procedure, hence the inter-macro eNB HO condition can be similar to, or more difficult than, the macro-macro HO condition. That is, for C-plane transition, the C/U-plane-split HO has low mobility robustness similar to the LTE-A macro-macro HO with single connectivity. This phenomenon was further verified by the result of the data interruption time per UE performing HOs with single and dual connectivity in [11].

To improve the HO robustness for C-plane transition to mobile users in the C/U-plane-split architecture, first, we require a natural and compatible setup to realize the features of a C/U-plane-split network. A potential solution is the 3GPP standardized dual-connectivity (DC) technique [1], [4], [12], which enables the superior and robust mobility management performances demonstrated in the previous studies [11], [13], [14]. However, their inter-macro eNB HOs operate the same as in [10], hence the problem of the inter-macro eNB HO was not addressed. The second potential solution is that we require an improved HO protocol design for the inter-macro eNB HO. From previous studies, there were heated discussions regarding improved HO protocol designs. One of the most robust methods is a kind of dual-link HO scheme [15]–[20] where a bi-casting concept, Carrier Aggregation (CA) technique, or coordination multi-point (CoMP) functionality is used to provide the two chances of an HO trigger and data transmission. Therefore, how to design the improved inter-macro eNB HO protocol, with the concept of a dual-link HO scheme, based on the DC setup is a challenge.

Combining both of the above ideas, in this paper we propose a DC-based prevenient HO scheme (PHO) to improve the robustness of the inter-macro eNB HO. Precisely, PHO is based on the 3GPP standardized DC technique to be equipped with the specific coordination functions different from previous dual-link HO schemes, for example, RRC HO signalling duplication and master-secondary role switch, between two macro eNBs to reduce the risk of HO failures (HOFs) and long service interruption time.

Moreover, we follow the definitions of the HOFs in the 3GPP LTE-A specification [21], which are close to the real testbed operations and inconsistent with those in the majority of the previous studies [13]–[20]. The difference is that the Radio Link Monitor (RLM) process, namely the Radio Link Failure (RLF) detection mechanism specified in 3GPP LTE-A, is not considered. According to the specification, the effect of an RLF on an HO procedure results in an HOF. The majority of studies analyzing the performance of HOF are based on simulation results [11], [22]–[26] and only a small number of studies provide theoretical analyses of HOF [27]–[29]. However, in these studies it remains difficult to analyze and recognize the association between the RLM and HO processes in detail. For example, both kinds of RLFs and HOFs can degrade mobility performance; however, they have different meanings. Thus, they must be highlighted and considered in the development of mobility improvement.

Thus, we develop the analytical expressions, which are based on recurrence relations, for the approximations of the successful LTE-A HO and PHO trigger probabilities. This also allows us to verify the simulation models of PHO and baseline scheme of LTE-A HO. To the best of our knowledge, this is the first analytical model for HO performance considering the association between the RLM and HO processes. In the results, we verify the analytical results against the simulation results and compare these with representative previous schemes to demonstrate the improvement of PHO. The contributions of this paper can be summarized as follows:

1) Design of a robust HO scheme leveraging the nature dual-connectivity setup to improve the inter-macro eNB HO performance in C/U-plane-split networks, for which we present elaborations on the proposed protocol stack and signaling flow.
2) Consideration for HOFs aligned with the LTE-A specification: the effect of an RLF on an HO procedure (i.e., the association between the RLM and HO processes), which is simplified or ignored in the majority of previous studies.
3) The first development of analytical expressions considering the association between the RLM and HO processes, where we derive approximations of the successful HO trigger probabilities for both the proposed scheme and LTE-A HO.
4) Discussion of the verification of the analytical results against the simulation results, of the comprehensive mobility performance metrics including the HOF and RLF rates, and of the comparison with the representative schemes of the previous literature.

II. Mobility Technical Details and Performance Modeling

In this section, we review the background of the HO process, RLM process, and their association. The latter two topics were typically not addressed in previous studies. Moreover, three related metrics, RLF, HOF, and ping-pong (PP) rates, considered in mobility performance evaluation, are reviewed. Any one of these metrics can influence the others.

A. Radio Link Monitor (RLM) Process

The process is executed on the UE side to detect an RLF, which means a connection loss between the UE and the serving eNB. The RLM process is based on Signal to Interference Noise Ratio (SINR) of the physical layer (L1) measurement whose sample rate is typically configured once every 10 ms (T_{L1}). Given a scenario where a UE has a serving eNB and a target eNB, the nth L1 measurement can be expressed as

$$M_{L1,n} = RSRP_{s,n} - RSRP_{t,n} \tag{1}$$

where $RSRP_{s,n}$ and $RSRP_{t,n}$ (in the unit dBm) are the nth Reference Signal Received Powers (RSRPs) received from the serving and target macro eNBs respectively.

As L1 measurements drops below a threshold Q_{out} for the duration of the radio problem detection period T_{detect}, a timer T_{310} begins. During T_{310}, the connection can be recovered and the timer T310 is canceled if consecutive N_{311} L1 measurements (equal to T_{311}) rise above a threshold Q_{in}, or the RLF occurs upon the expiry of the timer T310.

B. LTE-A Handover (HO) Process

The HO process is triggered by the serving eNB according to measurement reports sent from the UE. A UE's RRC layer (L3) samples the L1 measurements for averaging and sends a measurement report of a L3 measurement to the serving eNB at the end of every L3 sampling period T_{L3}. The nth L3 measurement $M_{L3,n}$ can be expressed as

$$M_{L3,n} = a\frac{\sum_{j=(n-1)N_{L3}+1}^{nN_{L3}} M_{L1,j}}{N_{L3}} + (1-a)M_{L3,n-1} \quad (2)$$

where $N_{L3} = \frac{T_{L3}}{T_{L1}}$ and is the number of L1 measurements during T_{L3}, and the weighting value a is a filter coefficient.

The HO trigger method commonly is based on the A3 event, which is defined as

$$-M_{L3,n} \geq H \quad (3)$$

where Hysteresis Margin H (in the unit dB) is the HO threshold. If condition (3) is achieved, the Time-to-trigger (TTT) timer on T_{TTT} will begin. If all the L3 measurements during the period of T_{TTT} achieve (3), the serving eNB will make a decision to initiate the HO procedure.

The LTE-A HO procedure consists of three phases, preparation, execution, and completion phases. First, in the preparation phase, the serving eNB requests the target eNB for HO admission and forwards the necessary UE context to the target eNB for preparing the HO at the target side. Assume that there are sufficient resources at any target eNB for each mobile user's HO in this paper. Thus, the target eNB returns a HO request acknowledge, which includes a dedicated random-access channel (RACH) preamble and the L3 message RRC Connection Reconfiguration including mobility control information (same as the HO command) to be forwarded by the serving eNB to the UE to perform the HO. In the execution phase, the UE detaches from the serving eNB and the data forwarding between the serving and target eNBs starts after the HO command is received by the UE. Then, the UE starts a L1/L2 random access procedure, where the UE performs synchronization to the target eNB and sends the dedicated RACH preamble to the target eNB to access it in a contention-free manner. After the UE successfully accesses the target eNB, the UE sends the RRC Connection Reconfiguration Complete message to the target eNB to confirm that the handover is completed and the bearers of C/U-planes between the UE and the target eNB are established successfully. Finally, in the completion phase, the downlink path switch at the serving gateway and resource release on the serving eNB are conducted.

An HOF is defined when the UE is unlikely to decode the received HO signal and its HO process is interrupted because of the degraded signal quality. That is, the effect of an RLF on an HO procedure can determine an HOF, although the RLM process is independent of the HO process. Four cases of HOF are defined in the 3GP document [21]:

1) An HOF in the TTT period: An RLF occurs during T_{TTT}.
2) An HOF in the preparation phase: An RLF occurs during the preparation phase (T_{pre}).
3) An HOF due to a lost HO command: The T310 timer remains active at the end of T_{pre}, which means that the following HO command at the beginning of the execution phase T_{exe} could be lost.
4) An HOF in the execution phase: All of the L1 measurements associated with the target eNB (e.g., $-M_{L1,n}$) during the period of T_{exe} drop below Q_{out}, which means that the random access process and the RRC connection setup could fail.

A PP effect is defined when a UE has handed over from the serving eNB to the target eNB and then handed over back to the serving eNB in a short period. This can result in more than two successful HOs, which are the unnecessary HOs and result in degraded throughput and significant signaling overhead. In the 3GPP document [21], the time from the point that a UE attaches to the target eNB successfully to the point that the UE attaches back to the serving eNB is referred to as Time of Stay (ToS). If the period of ToS is less than a configured value Minimum-Time-of-Stay (MTS), a PP effect occurs. The MTS is suggested to be one second.

III. Network Architecture

We adopt a C/U-plane-split network architecture similar to that adopted in [10] for a high-speed railway system, which is illustrated in Fig. 1. For clarity, we consider that there is an MR deployed in a train to represent a group of UEs. Furthermore, macro and micro eNBs are deployed along the track and are D_{macro} and D_{micro} away from the track respectively, where $D_{macro} > D_{micro}$. The inter-site distances between two macro eNBs and between two micro eNBs are R and r respectively. Each macro eNB controls three micro eNBs, one of which is centered with its macro eNB. A macro eNB connects to its subordinate micro eNBs and neighbor macro eNBs by means of X2 interface signalling.

To realize the C/U-plane-split in the architecture, the eNBs and MR are based on the DC technique of LTE-A Rel12 [1], which naturally supports the features of C/U-plane-split in terms of radio protocol architecture and network interface. In the next subsections, we introduce the C/U-plane-split and DC techniques.

A. C/U-Plane-Split

To provide spectrum extension and network density enhancements and even mitigate the signalling cost of mobility due to frequent HOs, the idea of C/U-plane-split was proposed. In a C/U-plane-split network, the signalling and data networks, which are referred to as C/U-planes respectively, are split per different eNBs' coverage sizes. The C-plane configured with a wide coverage facilitates mobility management and the guarantee of control signalling. The time for staying in a

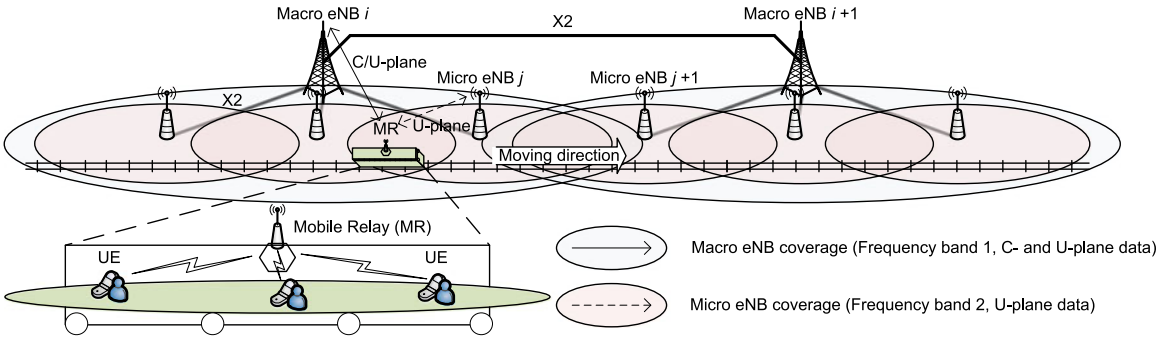

Fig. 1. System architecture.

wide-coverage area is long, hence a network coverage composed of wide-coverage areas is prone to reduce the possibility of frequent HOs and it is easy to consistently maintain and manage MRs' connections in the same coverage. The U-plane requires high data rate and flexibility in management, hence small coverage with a high data transmission rate fits a U-plane node well; a C-plane node covers and manages more than one U-plane nodes. Through this, cell-edge/hotspot throughput can be improved.

To map the C/U-plane-split to our architecture, the macro eNBs are responsible for both C/U-planes transmissions, which operate on the frequency band one below 2.5 GHz to provide large coverage and guarantee the reliability of message transmission (specially control signaling). To increase the system capacity in coverage of a macro eNB, micro eNBs are deployed within the macro eNB and responsible for U-plane transmission, which operates on the frequency band two above 2.5 GHz. This also means there is no interference between the macro and micro eNBs.

A macro eNB operates as a C-plane node and is responsible for all RRC procedures (e.g., system information, connection and mobility controls, and measurements) of the MRs, which connect to the macro eNB and its underlying micro eNBs. This means a macro eNB is also responsible for the RRC procedures between the MRs and its underlying micro eNBs. For example, MRs must transmit the measurement reports for the signal quality of the underlying micro eNBs to the macro eNB to identify the appropriate underlying micro eNB. Thus, the micro eNBs operate as dedicated U-plane nodes, which have no requirement to support cell-specific parameters and information such as primary/secondary synchronization signals (PSSs/SSSs), cell-specific reference signals (CRSs) and all types of system information blocks (SIBs). To enable the MRs to identify an underlying micro eNB and estimate the Channel State Information (CSI) for its bandwidth rather than that of the macro eNB, we adopt CSI reference signals (CSI-RSs) for the transmission of an underlying micro eNB. That is, the transmission from the underlying U-plane nodes can be regarded as the transmission of the addition of antenna ports, which are managed by their C-plane node. In terms of the mobility controls, there are two major types of handovers in a C/U-plane-split network:

1) Intra-macro eNB HO: The mobility between the underlying micro eNBs under the same macro eNB is referred to as the intra-macro eNB HO related to L1/L2 protocols only, where a MR attaches to a micro eNB through the LTE-A random access procedure. No RRC signaling is required in an intra-macro eNB HO procedure; hence, there are signaling savings and shorter latency can be achieved for the mobility in a C/U-plane-split network.
2) Inter-macro eNB HO: The mobility between macro eNBs mainly involves the macro-macro HO related to the C-plane transition. Further, the U-plane transition between the micro eNBs managed by different macro eNBs must follow the C-plane transition. Hence, even the micro-micro HO can be involved in an inter-macro eNB HO.

B. Dual Connectivity

The DC technique in 3GPP is a nature solution for a C/U-plane-split network to enhance the mobility robustness and improve the quality of services for cell edge users. With the DC technique, a UE is simultaneously served by two eNBs, which manage their own radio resource including C/U-planes and are interconnected with an X2-based backhaul. One of the eNBs is referred to as the master eNB (MeNB) providing C/U-plane transmissions for a UE; the other is referred to as the secondary eNB (SeNB) providing only U-plane transmission. Unlike inter-site carrier aggregation, the DC technique integrates an eNB as a small cell, not a remote radio head (RRH). Thus, the X2-based backhaul in the DC technique can be non-ideal and the eNBs can manage their radio resource independently for DC UEs. Naturally, using X2 interface signalling, inter-eNB signalling and coordination can be performed. To be more scalable for more scenarios, the MeNB and the SeNB can further form into a master cell group (MCG) and a secondary cell group (SCG) with multiple cells. Fig. 2 illustrates the DC radio protocol architecture of the specification. Three types of bearer, MCG bearer, SCG bearer, and split bearer are supported for a DC UE. U-plane traffic passes through the protocol layers of the MeNB and SeNB over the MCG and SCG bearers respectively, whereas U-plane traffic is split at the packet data convergence protocol (PDCP) layer of the MeNB, which is interconnected with the radio link control (RLC) layer of the SeNB, over the split bearer. Therefore, these types of bearers provide a C/U-plane-split network with the flexibility of U-plane traffic transmission. To fit the

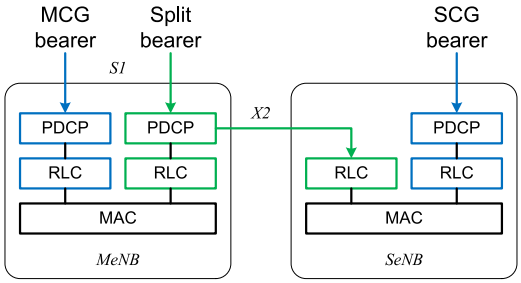

Fig. 2. Radio protocol architecture for the 3GPP dual connectivity.

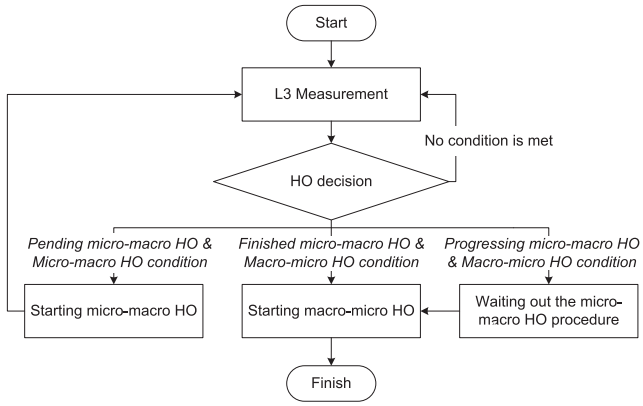

Fig. 3. State diagram of the proposed two-level HO trigger mechanism.

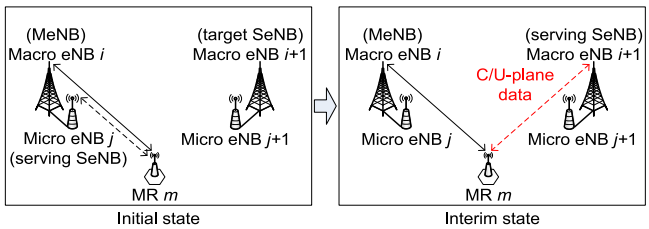

Fig. 4. Example of a micro-macro HO procedure.

proposed architecture where the subordinate micro eNBs connect to their macro eNB, not a serving gateway (SGW), U-plane traffic is transferred from a macro eNB (also MeNB) to its micro eNBs (also SeNBs) using the X2 interface. In terms of C-plane, the RRC layer is located in the MeNB and a signalling radio bearer (SRB) from the MeNB to a UE is always configured as the type of MCG bearer. This corresponds with the concept of C/U-plane-split. Moreover, the MeNB acts as a mobility anchor towards the core network for the served DC UEs. Consequently, U-plane traffic over any type of a bearer of a UE will be interrupted by C-plane transition during an MeNB handover from an eNB to another in the current 3GPP specification.

IV. Proposed Scheme

In this paper, we focus on the inter-macro eNB HO for C/U-plane-split networks in the high-speed railway scenario. On the basis of the protocol architecture and mobility in dual connectivity, we propose a prevenient handover (PHO) scheme that coordinates two consecutive macro eNBs to provide a robust HO. The PHO scheme includes a two-level HO trigger mechanism, micro-macro HO procedure (from the serving micro eNB to the target macro eNB), and macro-micro HO procedure (from the serving macro eNB to the target micro eNB). The micro-macro HO procedure makes the target macro eNB the SeNB in advance to support RRC HO signalling duplication in the state of dual connectivity to both serving and target macro eNBs. This improves the mobility robustness in an inter-macro eNB HO. Moreover, the next macro-micro HO procedure provides the mobility coordination of the C-plane transition of inter-macro eNB HO by means of the X2 interface signalling exchange; consequently, it effectively reduces the service interrupt time. In the following subsections, we elaborate on the three components of the PHO scheme.

A. Two-Level HO Trigger Mechanism

After an MR receives the L3 message Measurement Control, it initiates the two-level HO trigger mechanism. For simplicity, we assume that the measurement mechanism is always started before an inter-macro eNB HO. If every L3 measurement result meets the condition of PHO decision then the corresponding operation is performed, otherwise L3 measurement continues.

The micro-macro and macro-micro HO procedures are triggered in sequence in PHO; hence, we design a means of "two-level" HO conditions to trigger these respective HO procedures. The micro-macro and macro-micro HO procedures require respective HO trigger conditions. Both conditions are based on the rules of the A3 event and TTT as in LTE-A HO; however, we must prioritize the HO conditions to trigger the micro-macro HO procedure first. Thus, we design the micro-macro HO condition as a subset of the macro-micro HO condition by configuring the micro-macro and macro-micro HO conditions with the same Hysteresis Margin H, but with T_{TTT1} and T_{TTT2} respectively, where $T_{TTT1} < T_{TTT2}$. Hence the micro-macro HO procedure must be triggered before the macro-micro HO procedure.

Furthermore, we must consider the case that the macro-micro HO condition is met while the micro-macro HO procedure is in progress as another condition for the HO decision. As indicated in Fig. 3, the possible combinations of the HO conditions in the HO decision are classified into three cases.

B. Micro-Macro HO Procedure

The objective of the micro-macro HO procedure is to make the role of the SeNB for an MR changeover from the serving micro eNB to the target macro eNB. Thus, the MR can obtain the radio and bearer resources of the target macro eNB in advance by establishing dual connectivity to both the serving macro eNB and the target macro eNB.

Fig. 4 shows an example of the micro-macro HO procedure. In the initial state, an MR is configured for dual connectivity to macro eNB i and micro eNB j, which play the roles of the MeNB and SeNB respectively. At this moment, the U-plane data is transmitted through the MCG and split bearers via the MeNB and SeNB respectively. The MeNB configures the MR to feedback measurement reports of the radio-bearer channel quality. As the micro-macro HO procedure is pending and the

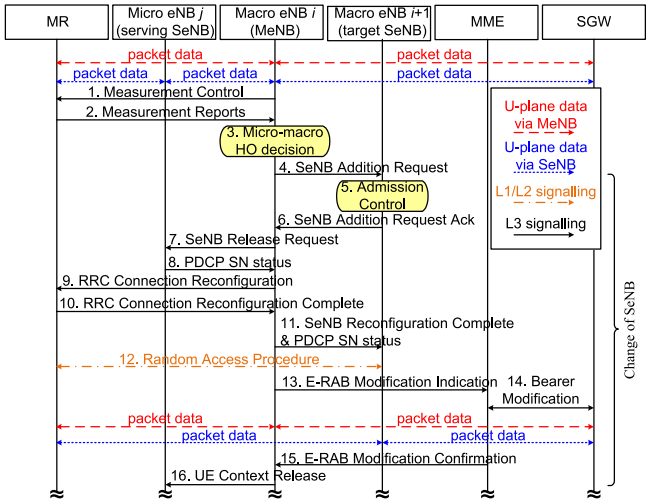

Fig. 5. Message flow diagram of a micro-macro HO procedure.

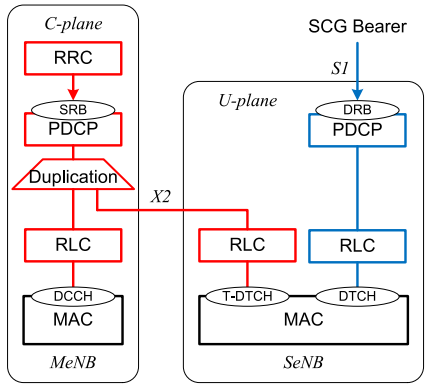

Fig. 6. Modified DC radio protocol architecture to support the functionality of RRC HO signalling duplication.

micro-macro HO condition is achieved, the micro-macro HO procedure is initiated by the MeNB. To allow the HO procedure to conform to the LTE-A specifications, we propose the adoption of the *change of SeNB* procedure, which is the existing DC operation in [1]. Thus, in the micro-macro HO procedure, the SeNB is changed from the serving micro eNB to the target macro eNB and the MR context is transferred in the same manner. Fig. 5 displays the message flow diagram of the micro-macro HO procedure in detail.

1) Interim State: After the target macro eNB becomes the SeNB, the dual connectivity to both the serving macro eNB and target macro eNB is established. This state we refer to as the interim state is indicated in the right subfigure in Fig. 4. According to the two-level HO trigger mechanism, the interim state can persist until the macro-micro HO condition is achieved. The MR has already connected with the target macro eNB, hence it can prefetch the radio and bearer resources of the target macro eNB. Further, the MR also can maintain both C/U-plane transmissions through the MCG and SCG bearers during the interim state.

In the event that in the interim state the channel quality has degraded below the micro-macro HO condition and remains above the macro-micro HO condition for a set time, the MeNB uses an interim timer configured with the duration of T_{inter}. This timer is designed to restore the dual connectivity configured in the interim state to the connectivity state configured prior to the micro-macro HO procedure. If the timer expires before the achievement of the condition of the macro-micro HO procedure, the MeNB performs the change of SeNB from the target macro eNB to the serving micro eNB. If the condition of macro-micro HO procedure is achieved, the timer also terminates.

2) RRC HO Signalling Duplication: Owing to the fact that an interim state immediately precedes the next macro-micro HO procedure, where C-plane transition occurs, it is natural to provide increased HO reliability under an interim state for the next C-plane transition. According to the four cases of HOF mentioned in Section II, the occurrence of RLF causing the failed reception of HO signalling at an MR during an HO procedure is the main reason for the occurrence of an HOF. According to the concept of the duplication of PDCP protocol data units (PDUs) for the control plane in the 5G new radio (NR) specification [30], we reduce the risk of HOFs using the transmit diversity for HO signalling. Thus, we propose a concrete RRC HO signalling duplication functionality, which is supported by the PDCP layer, to provide two MR reception opportunities for RRC HO signalling during an interim state. Specifically, the PDCP PDUs of the RRC HO messages are duplicated and then the originals and duplicates of those PDCP PDUs are transmitted to an MR through the MCG bearer and a dedicated split bearer respectively. Thus, RRC HO signalling duplication and the dedicated split bearer must be supported in the DC radio protocol architecture.

Fig. 6 displays the modified DC radio protocol architecture. We add a duplication function between the PDCP and RLC layers of the MeNB to duplicate PDCP PDUs transporting RRC HO messages. Further, a dedicated split bearer is established between the MeNB and SeNB over the X2 interface. In the SeNB, there is the corresponding RLC layer to receive the duplicates. According to the specification [1], the MeNB is responsible for the RRC to MRs and SRBs are always configured as the type of MCG bearer. Thus, RRC signalling only uses the radio resources of the MeNB. To ensure that the SeNB is responsible for U-plane transmissions only, the RLC PDUs transporting the duplicates must be transferred across a special logical channel, referred to as a transparent dedicated traffic channel (T-DTCH), to the MAC layer. A DTCH logical channel is used to transmit U-plane data in the LTE-A specifications. The MAC layer therefore can manage and transfer the RLC PDUs transporting the duplicates as U-plane data. That is, on the dedicated split bearer, the duplicates of RRC HO messages are transmitted transparently through the DTCH from the SeNB to a MR. Note that the T-DTCH has a higher priority for the duplicates of RRC HO messages over that of the other DTCHs from the SeNB to a MR. After the RRC connection reconfiguration of micro-macro HO completes, the MeNB and the SeNB have established a dedicated split bearer for RRC HO signalling duplication. Consequently, the MR can receive RRC HO messages and their duplicates from both the MeNB and the SeNB respectively.

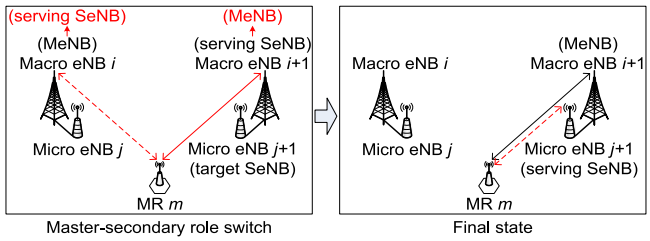

Fig. 7. Example of a macro-micro HO procedure.

C. Macro-Micro HO Procedure

To conclude the PHO after the completion of a micro-macro HO procedure, a macro-micro HO procedure is performed. It includes two sequential operations, a master-secondary role switch and change of SeNB, for respectively C-plane and U-plane transitions. Fig. 7 shows an example of the macro-micro HO procedure. As the macro-micro HO condition is achieved and the micro-macro HO procedure has completed, the MeNB makes the HO decision to trigger a macro-micro HO procedure. The first operation of a macro-micro HO procedure is introduced as follows:

Master-secondary role switch: The master-secondary role switch is the procedure for C-plane transition where the MeNB and the SeNB exchange the C-plane-related information associated to the MR context through the X2 interface. The purpose of this procedure is to upgrade the old SeNB to a new MeNB and downgrade the old MeNB to a new SeNB.

The random access procedure, which is inherent in the LTE-A HO procedure for C-plane transition, is omitted in the master-secondary role switch. Note handovers in LTE-A networks are 'hard' handovers (including the PHO) because of the characteristic of its flat architecture. A hard HO means that an MR's connection to the source cell is broken before a new connection is initiated to the target cell by the MR, thus there is a service interrupt time due to the C-plane transition during the handover. However, according to the results in [16], the service interrupt time of PHO can be reduced to approximately 10 ms by replacing the random access procedure with the X2 interface signalling exchange.

This is because the MR has prefetched the radio access information (L1 and L2 configurations) of the target macro eNB in the micro-macro HO procedure, in addition to the radio link between the MR and target macro eNB, which has previously been established. Then, the MR is configured with the role switch between the old MeNB and SeNB, via RRC signalling, by the old MeNB. Further, the MR remains in the interim state and as such, the RRC HO signalling duplication is functioning. The RRC connection configuration message for the role switch therefore is duplicated and forwarded to the MR to allow the transmit diversity to reduce the risk of HOFs before the C-plane transition succeeds. Note that if there is a mismatch between the target macro eNB and the final macro eNB for the micro-macro HO and the macro-micro HO respectively, it is possible to perform a fallback to the final macro eNB through an LTE-A HO procedure, instead of the sequential operations of the macro-micro HO.

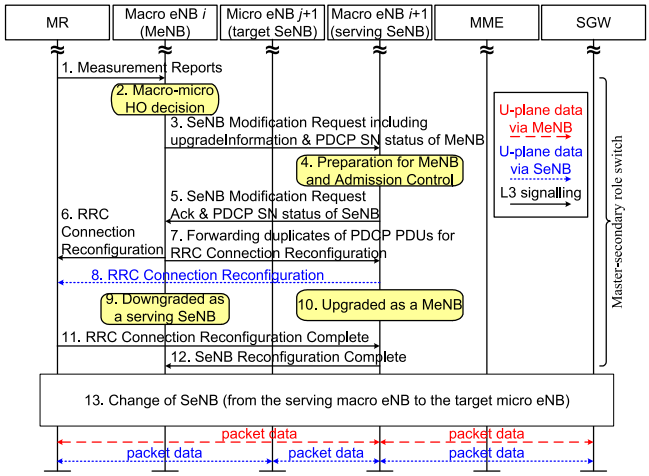

Fig. 8. Message flow diagram of a macro-micro HO procedure.

Then, the new MeNB performs the change of SeNB from the old macro eNB i to the target micro eNB $j+1$. Following the change of SeNB, the new MeNB (the serving macro eNB $i+1$) requests the old macro eNB i to release the radio and C-plane related resources associated to the MR context. Finally, by the means of the PHO scheme, the MR completes an inter-macro eNB HO, during which the dual-connectivity configuration of the MR has persisted to maintain the service continuity. The persistence of dual connectivity is the most significant difference between the PHO and C/U-plane-split HO scheme in [10].

We explain in detail the message flow of the macro-micro HO procedure in Fig. 8.

V. Analysis of Effect of RLF on LTE-A HO and PHO

To investigate the association between the RLM and HO processes, we derive the analytical expressions based on recurrence relations for the approximations of the successful LTE-A HO and PHO trigger probabilities.

A successful HO trigger probability is defined as the probability that an HO process is triggered and performed successfully. That is, there is no occurrence of exception (e.g., RLF or HOF) to interrupt the HO process. The probability depends on the fusion of the probabilities of RLF, HOF, and HO occurrences, which are based on the timer-based operations specified by 3GPP for the RLM and HO processes. The PHO scheme is an improved LTE-A HO scheme based on dual connectivity, to reduce the possibility of HOFs. Hence, we develop the base model of the LTE-A HO for the successful HO trigger probability first, and then extend this to PHO.

A. L1 and L3 Measurement Models

The probabilities of RLF and HO occurrences are dependent on L1 and L3 measurements respectively. The measurements are derived from the received RSRPs, thus we first start on a received RSRP at a certain time. We refer to the model of RSRP applied in [15]. An L1 measurement period is a minimum unit of measurement time in LTE-A, so the RSRP in the nth L1

measurement is shown as

$$RSRP_{i,n} = 10\log_{10}\left(\frac{P_d \Omega sh_{i,n}^2}{pl_{i,n}^2}\right), \quad (4)$$

where $i \in \{s,t\}$ stands for the serving and target eNBs respectively, P_d is the transmitted power, Ω is the multipath fading, $pl_{i,n}^2$ is the path loss, and $sh_{i,n}^2$ is the shadowing fading. As their network architecture is similar to the proposed one, where there are two macro eNBs responsible for RRC signalling. Therefore, based on their SINR model, the nth L1 measurement can be expressed as

$$M_{L1,n} = 10\log_{10}\frac{sh_{s,n}^2 pl_{t,n}^2}{pl_{s,n}^2 sh_{t,n}^2} = -(\triangle P_n + \triangle S_n), \quad (5)$$

where the serving and target macro eNBs have the same transmitted power and multipath fading. Hence, the remaining terms present the differences in the path loss and shadowing fading between the serving and target macro eNBs by $\triangle P_n$ and $\triangle S_n$ respectively. In terms of the shadowing fading, $10\log_{10}sh_{s,n}^2$ and $10\log_{10}sh_{t,n}^2$ are independent normal random variables with a zero mean and respective variances $\sigma_{s,n}^2$ and $\sigma_{t,n}^2$. Thus, $\triangle S_n$ is an independent normal random variable with a zero mean and variance $\sigma_{s,n}^2 + \sigma_{t,n}^2$.

We assume that L1 and L3 measurements are independent because of separate RLM and HO processes. Thus, the filter coefficient a of L3 measurement is configured to one such that two L3 measurements are independent. Therefore, the nth L3 measurement can be expressed as

$$M_{L3,n} = \frac{\sum_{i=(n-1)N_{L3}+1}^{nN_{L3}} -\triangle P_i - \triangle S_i}{N_{L3}}, \quad (6)$$

where N_{L3} is the number of L1 measurements in an L3 measurement.

B. Successful LTE-A HO Trigger Probability

Fig. 9 displays three events ①, ② and ③, which indicate necessary conditions of a successful LTE-A HO trigger. The event ① is that a condition of TTT is achieved at $M_{L3,n}$, which means $-M_{L3,i} \geq H, n - N_{TTT\_L3} - 1 < i \leq n$, where $N_{TTT\_L3} = \frac{T_{TTT}}{T_{L3}}$. We define a general probability that a condition of TTT is achieved at $M_{L3,t}$ and the first L3 measurement started at $M_{L3,s}$ as the equation (7), shown at the bottom of this page, where $TTT_{type}, \overline{TTT}_{type} \in \{T_{TTT1}, T_{TTT2}\}$. According to the proposed two-level HO trigger mechanism of PHO, there are the two lengths of TTT, T_{TTT1} and T_{TTT2}. TTT_{type} stands for a TTT period, during which all of the L3 measurements remain below the threshold $-H$, whereas $\overline{TTT}_{type}$ stands for a TTT period, during which all of the L3 measurements do not remain below $-H$. In the region defined by (7a), the achievement of the condition of TTT occurs at the beginning of the L3 measurement process. It indicates that the L3 measurements remaining below $-H$ start from the sth to the tth L3 measurement. We express the probability of the nth L3 measurement being below $-H$ as

$$\begin{aligned} m_n &= P(-M_{L3,n} \geq H) = P\left(\sum_{i=(n-1)N_{L3}+1}^{nN_{L3}} M_{L1,i} \leq N_{L3}H\right) \\ &= P\left(\sum_{i=(n-1)N_{L3}+1}^{nN_{L3}} \triangle S_i \geq -N_{L3}H - \sum_{i=(n-1)N_{L3}+1}^{nN_{L3}} \triangle P_i\right) \\ &= Q\left(\frac{-N_{L3}H - \sum_{i=(n-1)N_{L3}+1}^{nN_{L3}} \triangle P_i}{\sqrt{\sum_{i=(n-1)N_{L3}+1}^{nN_{L3}} \sigma_{s,i}^2 + \sigma_{t,i}^2}}\right). \end{aligned} \quad (8)$$

In (7b), the L3 measurements remaining below $-H$ start from the $(t - \frac{TTT_{type}}{T_{L3}})$th to the tth L3 measurement. The $(t - \frac{TTT_{type}}{T_{L3}} - 1)$th L3 measurement must be above $-H$ to ensure that the condition of TTT begins from the $(t - \frac{TTT_{type}}{T_{L3}})$th L3 measurement. In addition, no condition of TTT has been achieved before the $(t - \frac{TTT_{type}}{T_{L3}} - 1)$th L3 measurement. We determine the complement of the probability of condition of TTT occurring before the $(t - \frac{TTT_{type}}{T_{L3}} - 1)$th L3 measurement. That is $1 - P_{HOT}(s,t,T_{type})$ in (7), and includes all possibilities that a condition of TTT with the length of $\frac{TTT_{type}}{T_{L3}}$ is achieved during a period from the sth to the tth L3 measurement. Therefore,

$$P_{HOT}\left(s,t,\frac{T_{type}}{T_{L3}}\right) = \begin{cases} \sum_{i=s}^{t} & P_H\left(s,i,\frac{T_{type}}{T_{L3}},\frac{T_{type}}{T_{L3}}\right), \quad \text{if } t-s \geq \frac{T_{type}}{T_{L3}} \\ 0, & \text{otherwise.} \end{cases} \quad (9)$$

Based on the equation (7), we configure the length of TTT to T_{TTT2} for the LTE-A HO. Thus, the probability of the event ① is $P_H(1,n,\frac{T_{TTT2}}{T_{L3}},\frac{T_{TTT2}}{T_{L3}})$.

Next, the event ② is that no exceptions have occurred before $M_{L1,nN_{L3}+N_{pre}+1}$, where the types of exception include the RLF and the three cases of HOF: HOFs in T_{TTT}, in T_{pre}, and due to a lost HO command. In short, the event means no RLF has occurred before the beginning of HO execution phase and no HOF due to a lost HO command has occurred. Thus, we define a general probability that no exceptions have occurred be-

$$P_H\left(s,t,\frac{TTT_{type}}{T_{L3}},\frac{\overline{TTT}_{type}}{T_{L3}}\right) = \begin{cases} \prod_{i=s}^{t} m_i, & \text{if } t = s + \frac{TTT_{type}}{T_{L3}} \quad (7a) \\ \left(1 - P_{HOT}\left(s, t - \frac{TTT_{type}}{T_{L3}} - 2, \frac{\overline{TTT}_{type}}{T_{L3}}\right)\right) & \\ \quad \times \left(1 - m_{t-\frac{TTT_{type}}{T_{L3}}-1}\right) \prod_{i=t-\frac{TTT_{type}}{T_{L3}}}^{t} m_i, & \text{if } t > s + \frac{TTT_{type}}{T_{L3}} \quad (7b) \\ 0, & \text{otherwise.} \quad (7c) \end{cases}$$

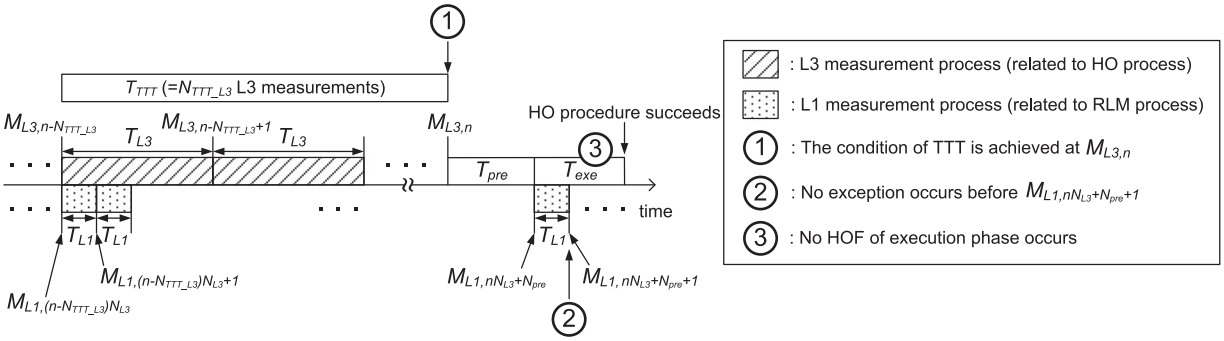

Fig. 9. Analysis illustration of the LTE-A HO procedure.

fore t and the first L3 measurement has started at $M_{L3,s}$ as the equation (10), shown at the bottom of this page, where $N_{detect} = \frac{T_{detect}}{T_{L1}}$, $N_{310} = \frac{T_{310}}{T_{L1}}$, and $L_{type} \in \{l_s, l_t\}$. L_{type} is the type of eNB, which a MR measures via the procedure of L1 measurements, thus l_s and l_t stand for the serving and target macro eNBs respectively. In the region defined by (10a), the time duration from the sth to the tth L1 measurement is insufficient to run a detection timer and T310 timer. Thus, all HOF types, except the HOF due to the lost HO command, cannot be detected. Using a complement rule, the complement of the probability that no HOF due to the lost HO command has occurred is shown as the equation (11) shown at the bottom of this page, where the equations (11a)–(11d) correspond to the equations (10a) and (10b) according to their regions.

In the region defined by (11a), the time period of $t - s$ is sufficient to achieve the condition that L1 measurements drop below Q_{out} for a period of T_{detect} with reference to the beginning of the sth L1 measurement. This is called a condition of radio problem detection and is expressed as

$$P_D(s, L_{type}) = \prod_{i=s}^{s+N_{detect}} q_i^{(out, L_{type})}, \tag{12}$$

where the probability that the ith L1 measurement with respect to the serving macro eNB l_s is below Q_{out} is defined as

$$q_i^{(out,l_s)} = P(M_{L1,i} < Q_{out}) = Q\left(\frac{-Q_{out} - \triangle P_i}{\sqrt{\sigma_s^2 + \sigma_t^2}}\right), \tag{13}$$

while the probability that the ith L1 measurement with respect to the target macro eNB l_t is below Q_{out} is defined as

$$q_i^{(out,l_t)} = P(-M_{L1,i} < Q_{out}) = 1 - Q\left(\frac{Q_{out} - \triangle P_i}{\sqrt{\sigma_s^2 + \sigma_t^2}}\right). \tag{14}$$

$$P_{EX}(s,t,L_{type}) = \begin{cases} 1 - P_{lost}(s,t,L_{type}), & \text{if } N_{detect} \le t-s < N_{detect} + N_{310} \quad (10a) \\ 1 - P_{RLF}(s,t-1,L_{type}) - P_{lost}(s,t,L_{type}), & \text{if } N_{detect} + N_{310} \le t-s \quad (10b) \\ 1, & \text{if } t-s < N_{detect}. \quad (10c) \end{cases}$$

$$P_{lost}(s,t,L_{type}) = \begin{cases} P_D(s,L_{type}), & \text{if } t-s = N_{detect} \quad (11a) \\ P_{lost}(s, s+N_{detect}, L_{type}) + \sum_{i=s}^{t-N_{detect}} P_{QD}(i, L_{type}), & \text{if } N_{detect} < t-s < N_{detect} + N_{311} \quad (11b) \\ P_{lost}(s, s+N_{detect}+N_{311}-1, L_{type}) \\ \quad + \sum_{i=s}^{t-N_{detect}-N_{311}} (1 - P_{lost}(s,i,L_{type})) \\ \quad \times P_{QDR}(i,t,L_{type}) \\ \quad + \sum_{i=t-N_{detect}-N_{311}+1}^{t-N_{detect}} (1 - P_{lost}(s,i,L_{type})) P_{QD}(i,L_{type}), & \text{if } N_{detect} + N_{311} \le t-s < N_{detect} + N_{310} \quad (11c) \\ P_{lost}(s, s+N_{detect}+N_{310}-1, L_{type}) \\ \quad + \sum_{i=t-N_{detect}-N_{310}-1}^{t-N_{detect}-N_{311}} P_{EX}(s,i,L_{type}) \\ \quad \times P_{QDR}(i,t,L_{type}) \\ \quad + \sum_{i=t-N_{detect}-N_{311}+1}^{t-N_{detect}} P_{EX}(s,i,L_{type}) P_{QD}(i,L_{type}), & \text{if } N_{detect} + N_{310} \le t-s \quad (11d) \\ 0, & \text{otherwise.} \quad (11e) \end{cases}$$

A condition of radio problem detection is achieved at the $(s + N_{detect})$th L1 measurement, which the beginning of the HO execution phase is next to.

In the region defined by (11b), the L1 measurement before the duration of a successful condition of radio problem detection (where it is defined by (12) must be above the threshold of Q_{out} to ensure the length of the successful condition of radio problem detection not being longer than the length of N_{detect}. Therefore,

$$P_{QD}(s, L_{type}) = (1 - q_s^{(out,L_{type})}) \prod_{i=s+1}^{s+N_{detect}} q_i^{(out,L_{type})}. \tag{15}$$

In addition to (15), the previous state of $P_{lost}(s, s+N_{detect}, L_{type})$ indicated by (11a) is included in (11b).

In the region defined by (11c), the time period of $t - s$ is sufficient to run a T_{detect} timer with a T311 timer rather than a T310 timer. Thus, no HOF due to a lost HO command has occurred before the $(t - N_{detect} - N_{311} + 1)$th L1 measurement. That is indicated by $1 - P_{lost}(s, i, L_{type})$ in (11c). In addition, the T310 timer can be canceled when consecutive N_{311} L1 measurements are above the threshold of Q_{in} in incomplete duration of T310 timer. Thus, the connection can be recovered. After a condition of radio problem detection is achieved, given the next incomplete duration of T310 timer is sufficient to run a T311 timer, the complement of the probability that there is no connection recovered between the sth and tth L1 measurement is expressed as the equation (16), shown at the bottom of this page, where it is calculated by changing the T_{detect} timer and Q_{out} threshold in (11a) and (11b) into the T_{311} timer and Q_{in} threshold. Thus, $q_i^{(j,l_s)} = P(M_{L1,i} < Q_j)$ and $q_i^{(j,l_t)} = P(-M_{L1,i} < Q_j)$, where $j \in \{out, in\}$ stands for the use of Q_{out} or Q_{in} threshold. Consequently, in (11c), P_{QDR} is a combination between P_{QD} and the equation (16), and it is expressed as

$$P_{QDR}(s, t, L_{type}) = (1 - q_s^{(out,L_{type})}) \prod_{i=s+1}^{s+N_{detect}} q_i^{(out,L_{type})} \times (1 - P_{RLR}(s + N_{detect} + 1, t, L_{type})). \tag{17}$$

In other case that incomplete duration of T310 timer is insufficient to run a T311 timer, P_{QD} therefore is included in (11c). Also, the previous state of $P_{lost}(s, s + N_{detect} + N_{311} - 1, L_{type})$ indicated by (11b) is included in (11c).

In (10b), all HOF types cannot occur during the time period of $t - s$, which is sufficient to run a detection timer and T310 timer. Thus, we present the probability of the event by using its complement, which includes $P_{RLF}(s, t-1, L_{type})$ and $P_{lost}(s, t, L_{type})$. The probability including all possibilities that an RLF has occurred before the $(v + 1)$th L1 measurement and an RLM process started at the uth L1 measurement is shown as the equation (18) at the bottom of the next page. In (18a), the length of $v - u$ is equal to the length of a T_{detect} timer and T310 timer. Thus, an RLF occurs at the beginning of an HO procedure if the condition of radio problem detection is achieved and the connection is not recovered in the following duration of T310 timer. In (18b), a RLF occurs within the duration of $v - u$, which is longer than the length of a T_{detect} timer and T310 timer. Before the duration of a successful condition of radio problem detection, the L1 measurement must be above the threshold of Q_{out}; after which, no connection is recovered in the following duration of T310 timer. Thus, P_{QDR} is included in (18b). Furthermore, the case that no HOF has occurred before that L1 measurement is represented by P_{EX}. The previous state of $P_{RLF}(u, u + N_{detect} + N_{310}, L_{type})$ indicated by (18a) is included in (18b).

In terms of P_{lost} in (10b), according to the length of $t - s$ it is indicated by (11d). The equation (11d) is with the similar concept in (11c), but the difference is an additional probability $P_{EX}(s, i, L_{type})$ before P_{QDR}. It represents the probability that no HOF has occurred before ith L1 measurement in (11d). Thus, in (11c), $(1 - P_{lost}(s, i, L_{type}))$ represents the probability that no HOF due to the lost command has occurred before ith L1 measurement.

Based on the equation (10), the probability of the event ② is $P_{EX}(1, \frac{nT_{L3}}{T_{L1}} + N_{pre} + 1, l_s)$, where $N_{pre} = \frac{T_{pre}}{T_{L1}}$.

The event ③ is that all of the L1 measurements associating with the target eNB during an execution phase T_{exe} drop below Q_{out}. The probability of the event ③ is shown as

$$P_{exe}(n) = \prod_{i=nN_{L3}+N_{pre}+1}^{nN_{L3}+N_{pre}+N_{exe}} q_i^{(out,l_t)}, \tag{19}$$

$$P_{RLR}(s, t, L_{type}) = \begin{cases} \prod_{i=s}^{s+N_{311}-1}(1 - q_i^{(in,L_{type})}), & \text{if } t - s = N_{311} - 1 \\ P_{RLR}(s, s + N_{311} - 1, L_{type}) & \\ \quad + \sum_{i=s}^{t-N_{311}} q_i^{(in,L_{type})} \prod_{j=i+1}^{i+N_{311}}(1 - q_j^{(in,L_{type})}), & \text{if } N_{311} < t - s + 1 \le 2N_{311} \\ P_{RLR}(s, s + 2N_{311} - 1, L_{type}) & \\ \quad + \sum_{i=s+N_{311}}^{t-N_{311}}(1 - P_{RLR}(s, i-1, L_{type}))q_i^{(in,L_{type})} \prod_{j=i+1}^{i+N_{311}}(1 - q_j^{(in,L_{type})}), & \text{if } t - s > 2N_{311} - 1 \\ 0, & \text{otherwise.} \end{cases} \tag{16}$$

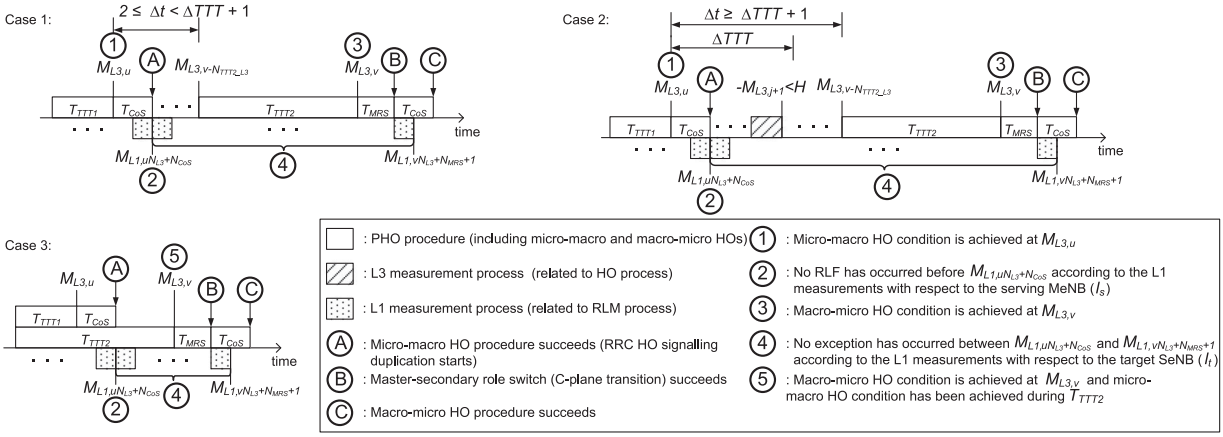

Fig. 10. Analysis illustration of the PHO procedure.

where $N_{exe} = \frac{T_{exe}}{T_{L1}}$. Note that $L_{type} = l_t$ stands for checking the L1 measurements with respect to the target macro eNB during an execution phase.

Finally, the successful LTE-A HO trigger probability at the nth L3 measurement is shown as

$$P_{HO}(n) = P_H\left(1, n, \frac{T_{TTT2}}{T_{L3}}, \frac{T_{TTT2}}{T_{L3}}\right)(1 - P_{exe}(n)) \times P_{EX}\left(1, \frac{nT_{L3}}{T_{L1}} + N_{pre} + 1, l_s\right). \quad (20)$$

C. Successful PHO Trigger Probability

Fig. 10 shows three cases of a successful PHO trigger, which are categorized by the duration, $\triangle t = v - u$, between the uth L3 measurement when a micro-macro HO condition is achieved once and the vth L3 measurement when a macro-micro HO condition is achieved later. These cases include the events ①–⑤ that stand for the conditions of their achievement, whereas the events Ⓐ, Ⓑ and Ⓒ indicate the completions of a micro-macro HO procedure, master-secondary role switch, and macro-micro HO procedure, respectively.

The probability of the case 1 is shown at the bottom of the page in (21a), where $\triangle TTT = T_{TTT2} - T_{TTT1}$. The first condition

$$P_{RLF}(u, v, L_{type}) = \begin{cases} P_D(u, L_{type}) & \\ \times(1 - P_{RLR}(u + N_{detect}, u + N_{detect} + N_{310}, L_{type})), & \text{if } v - u = N_{detect} + N_{310} \quad (18a) \\ P_{RLF}(u, u + N_{detect} + N_{310}, L_{type}) & \\ + \sum_{i=u}^{v - N_{detect} - N_{310}} P_{EX}(u, i, L_{type}) & \\ \times P_{QDR}(i, i + N_{detect} + N_{310} + 1, L_{type}), & \text{if } v - u > N_{detect} + N_{310}. \quad (18b) \end{cases}$$

$$P_{PHO}(u, v) = \begin{cases} P_H(1, u, \frac{T_{TTT1}}{T_{L3}}, \frac{T_{TTT1}}{T_{L3}}) P_H(u + 1, v, \frac{T_{TTT2}}{T_{L3}}, \frac{T_{TTT2}}{T_{L3}}) & \\ \quad \times P_{EX}(uN_{L3} + N_{CoS} + 1, vN_{L3} + N_{MRS} + 1, l_t) & \\ \quad \times(1 - P_{RLF}(1, uN_{L3} + N_{CoS}, l_s)), & \text{if } 2 \le \triangle t < \triangle TTT + 1 \quad (21a) \\ P_H(1, u, \frac{T_{TTT1}}{T_{L3}}, \frac{T_{TTT1}}{T_{L3}}) & \\ \quad \times \sum_{j=u}^{u + \triangle TTT - 1} \prod_{i=u+1}^{j} m_i(1 - m_{j+1}) P_H(j + 2, v, \frac{T_{TTT2}}{T_{L3}}, \frac{T_{TTT2}}{T_{L3}}) & \\ \quad \times P_{EX}(uN_{L3} + N_{CoS} + 1, vN_{L3} + N_{MRS} + 1, l_t) & \\ \quad \times(1 - P_{RLF}(1, uN_{L3} + N_{CoS}, l_s)), & \text{if } \triangle t \ge \triangle TTT + 1 \quad (21b) \\ P_H(1, v, \frac{T_{TTT2}}{T_{L3}}, \frac{T_{TTT1}}{T_{L3}}) & \\ \quad \times P_{EX}(uN_{L3} + N_{CoS} + 1, vN_{L3} + N_{MRS} + 1, l_t) & \\ \quad \times(1 - P_{RLF}(1, uN_{L3} + N_{CoS}, l_s)), & \text{if } u - \frac{T_{TTT1}}{T_{L3}} = v - \frac{T_{TTT2}}{T_{L3}} \quad (21c) \\ 0, & \text{otherwise.} \quad (21d) \end{cases}$$

indicated by ①is that a micro-macro HO condition is achieved at the uth L3 measurement for the first time, which is expressed as $P_H(1, u, \frac{T_{TTT1}}{T_{L3}}, \frac{T_{TTT1}}{T_{L3}})$. The second condition indicated by ②is that no RLF has occurred before the completion of change of SeNB from the serving micro eNB to the target macro eNB, where the RLM process depends on L1 measurements with respect to the MeNB (the serving macro eNB). That is, the connectivity to the MeNB responsible for the C-plane signalling will not be interrupted by a RLF before the event ②. Thus, this condition is expressed as $1 - P_{RLF}(1, uN_{L3} + N_{CoS}, l_s)$, where N_{CoS} is the number of L1 measurements in the period of change of SeNB. When change of SeNB is complete, the event Ⓐ occurs and the functionality of RRC HO signalling duplication begins. The third condition indicated by ③ is that a macro-micro HO condition is achieved at the vth L3 measurement and the first L3 measurement of this condition achievement began after the achievement of the previous micro-macro HO condition, and expressed as $P_H(u + 1, v, \frac{T_{TTT2}}{T_{L3}}, \frac{T_{TTT2}}{T_{L3}})$. Then, in a macro-micro procedure, a master-secondary role switch and change of SeNB from the serving macro eNB to the target micro eNB occur sequentially. The ends of these events are indicated by Ⓑ and Ⓒ respectively. The final condition indicated by ④is that no exception has occurred during an interim state (between the event Ⓐ and the beginning of change of SeNB). It is expressed as $P_{EX}(uN_{L3} + N_{CoS} + 1, vN_{L3} + N_{MRS} + 1, l_t)$, where N_{MRS} is the number of L1 measurements in the period of the master-secondary role switch. The phase of a master-secondary role switch can be compared to a preparation phase in LTE-A HO, because both master-secondary role switch and preparation phases consist of a similar sequence of operations, including MR context exchanges for the C-plane transition and sending a RRC Connection Reconfiguration message (equal to a HO command). Thus, an exception (including the type of an HOF due to a lost HO command) can be applied to the phase of a master-secondary role switch like a preparation phase. The functionality of RRC HO signalling duplication works during the interim state; however, the only way to fail PHO is that an exception regarding the target macro eNB (SeNB) occurs. This is because the target macro eNB (SeNB) will be the new MeNB by a master-secondary role switch and the connectivity to that macro eNB must be maintained until the beginning of the master-secondary role switch. Furthermore, there is no HOF in an execution phase in a PHO procedure, because C-plane transition in PHO is achieved by the means of an X2 interface signalling exchange, rather than a random access process and RRC connection setup.

The probability of the case 2 is shown in (21b). It is similar to the form in (21a), but the L3 measurement $M_{L3,j+1}$ must be above the threshold $-H$ before the first L3 measurement of this condition achievement ③. This ensures the condition ① ($-M_{L3,i} \geq H$, where $u - \frac{T_{TTT1}}{T_{L3}} \leq i \leq u$) has not been extended as the condition ③($-M_{L3,i} \geq H$, where $u - \frac{T_{TTT1}}{T_{L3}} \leq i \leq u + \frac{T_{TTT2} - T_{TTT1}}{T_{L3}}$).

The probability of the case 3 is shown in (21c) without the probabilities of the conditions ① and ③. In this case, the first L3 measurement of the condition achievement ① is the same as that of the condition ③. This means the micro-macro HO condition has been achieved during the period of T_{TTT2}. In short, a condition for the period of T_{TTT2} is achieved at the vth L3 measurement and no condition for the period T_{TTT1} has been achieved before the $(v - \frac{T_{TTT2}}{T_{L3}} - 1)$th L3 measurement. This new condition is indicated by ⑤and its probability is expressed as $P_H(1, v, \frac{T_{TTT2}}{T_{L3}}, \frac{T_{TTT1}}{T_{L3}})$.

TABLE I
DEPLOYMENT PARAMETERS

Parameters		Value
Number of	macro eNBs	2
	micro eNBs	4
Train Speed		360 km/h
Distance between	macro eNBs (R)	4.8 km
	micro eNBs (r)	1.6 km
Distance between	a macro eNB and the track (D_{macro})	50 m
	a micro eNB and the track (D_{micro})	2 m
Frequency band of	macro eNB	0.9 GHz
	micro eNB	2 GHz
Transmitted power of	macro eNB	37 dBm
	micro eNB	30 dBm
Antenna height of	macro eNB (h_{macro})	30 m
	micro eNB (h_{micro})	5 m
	MR (h_{mr})	2.5 m
Shadow Fading Std. σ,	if 10 (m) $< d <$ d_{BP}	4
	if $d_{BP} < d <$ 10000 (m)	6

VI. SIMULATION RESULTS

We developed a time-driven simulator to investigate the performance of PHO affected by the RLM process in the architecture displayed in Fig. 1. The velocity of the train is assumed to be 360 km/hr. To focus on the performance of the type of inter-macro eNB HO, the starting point of the train is aligned with the macro eNB i and the micro eNB $j - 1$ at the abscissa zero. We refer to the propagation scenario of the rural moving network in the Wireless World Initiative New Radio (WINNER) II document [31] for the deployment parameters and the path-loss model. The deployment parameters are presented in Table I.

For consistency with the proposed analytical models, based on the channel model adopted in [15] for the high-speed rail scenario, a single-path fading channel and independent log-normal distribution of shadow fading are considered in our simulation.

In addition to the verification of the analytical results of the LTE-A HO and PHO against those obtained with simulations, we compared the PHO with the LTE-A HO and two representative previous schemes on multiple mobility performance metrics. The two previous schemes are the HO schemes in [10] and [15]; we used CU-split HO and Dual-link HO to represent them respectively. All of the HO schemes operate with the RLM process in simulations. In terms of the settings for all of the HO schemes and the RLM process, we adopted the standard configurations available in [21]; the parameters are listed in Table II.

To confirm the verification of the analytical model, we compared the analytical results of average successful LTE-A HO and PHO trigger probabilities (as defined in Section V-B and Section V-C respectively) with the results obtained from our simulator. We considered different lengths of T_{TTT} and

TABLE II
SIMULATION PARAMETERS

Parameters	Value
L1 Sampling Period (T_{L1})	10 ms
L3 Sampling Period (T_{L3})	40 ms
Minimum Time of Stay (MTS)	1 s
HO Preparation Period (T_{pre})	50 ms
HO Execution Period (T_{exe})	40 ms
Period of Change of SeNB (T_{CoS})	90 ms
Period of Master-secondary Role Switch (T_{MRS})	10 ms
Detection Period (T_{detect})	40 ms
Q_{out}	-8 dB
Q_{in}	-6 dB
T_{310}	200 ms
T_{311}	20 ms
Hysteresis Margin (H)	3, 5 dB

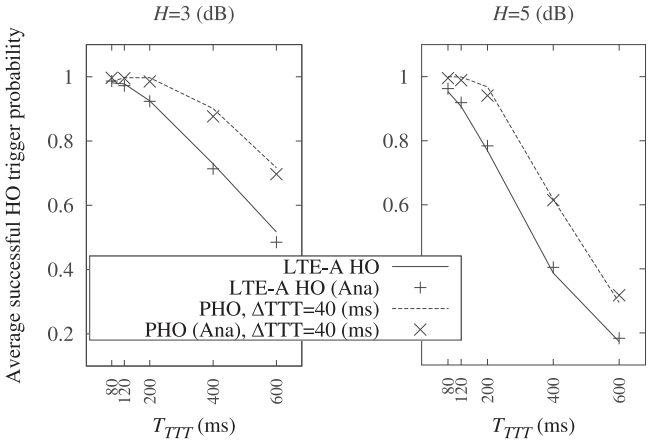

Fig. 11. Comparison of average successful LTE-A HO and PHO trigger probability between the analytical and simulation results.

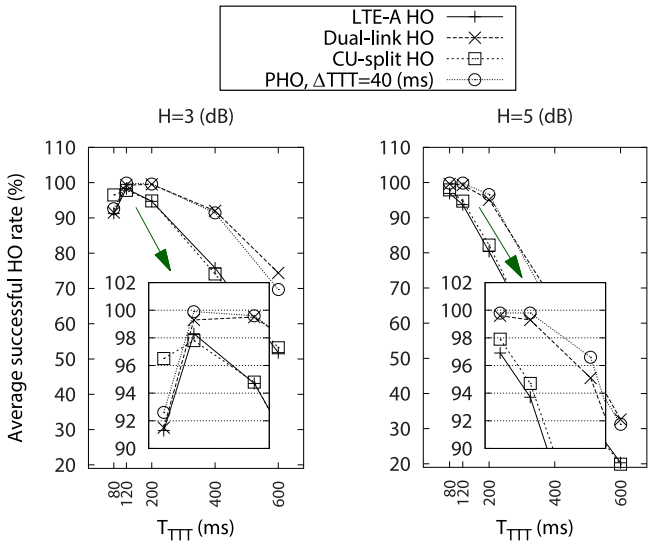

Fig. 12. Performance comparison of average successful HO rate among LTE-A HO, Dual-link HO, CU-split HO, and PHO schemes.

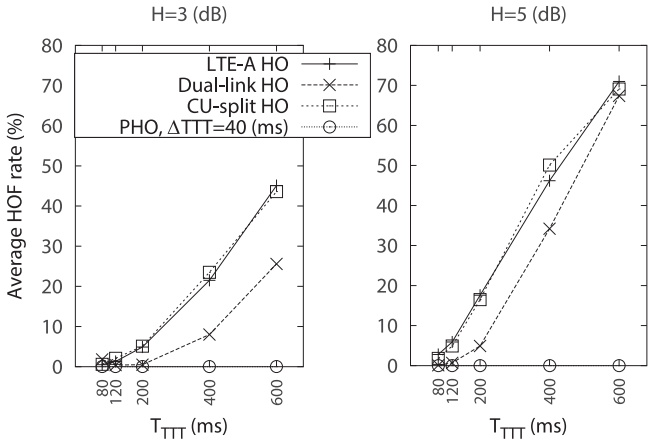

Fig. 13. Performance comparison of average HO failure (HOF) rate among LTE-A HO, Dual-link HO, CU-split HO, and PHO schemes.

different thresholds of H in both settings of LTE-A HO and PHO. Note that we could consider the timer on T_{TTT2} in the PHO as a TTT timer, because in the proposed analytical models we configure the length of T_{TTT} in the LTE-A HO to the same length of T_{TTT2}. Thus, the length of T_{TTT1} in PHO was equal to $T_{TTT} - \triangle TTT$. The results of average successful LTE-A HO and PHO trigger probabilities are displayed in Fig. 11, where the data for the analytical models are identified via "Ana". The proposed analytical models for those probabilities were similar to our simulation results. This means the analytical and simulation models corresponded. Therefore, the following performance evaluation of the different HO schemes is presented using simulations.

Fig. 12 displays the results of the average successful HO rate. The average successful HO rate is different from the average successful HO trigger probability. The average successful HO rate excludes the PP effects, the RLFs, and the HOFs, whereas the average successful HO trigger probability excludes the RLFs and the HOFs only. As the HO threshold of H increased, the average successful HO rate decreased more sharply in all of the HO schemes. We can see that Dual-Link HO and PHO have the similar average successful HO rates; however, look closely in the key region. PHO still outperformed Dual-link HO and achieved the higher average successful handover rate, approaching 100%. Further, when $H = 5$ dB, LTE-A HO and CU-split HO exhibited similar average successful HO rates. Over the set of all configurations, PHO realized a higher peak success rate than Dual-link HO. This is due to the higher average HOF rate in Dual-link HO. The reason is that the transmit diversity for HO signalling provided by PHO is better than the time diversity offered by the two chances of an HO trigger provided by Dual-link HO. When $H = 3$ dB and $T_{TTT} = 80$ ms, CU-split HO outperformed the other HO methods, as it has the lowest PP rate. However, as T_{TTT} increased, PHO and Dual-link HO outperformed CU-split HO and LTE-A HO.

Fig. 13 shows the results of the average HOF rate. Only PHO had no HO failure. This is because no RLF occurred during the interim state, where there is support of RRC HO signalling duplication. Thus, the advantage of DC is evident. Furthermore,

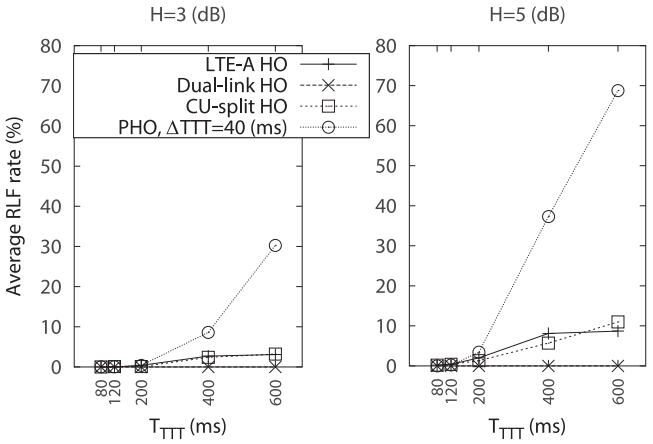

Fig. 14. Performance comparison of average radio link failure (RLF) rate among LTE-A HO, Dual-link HO, CU-split HO, and PHO schemes.

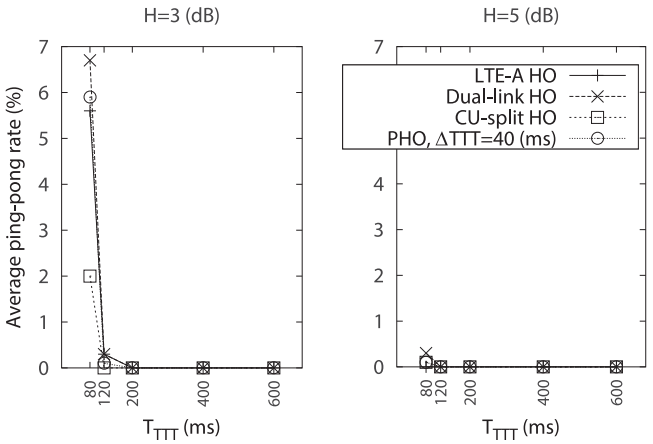

Fig. 15. Performance comparison of average ping-pong (PP) rate among LTE-A HO, Dual-link HO, CU-split HO, and PHO schemes.

LTE-A and CU-split HOs exhibit the highest HO failure rates as they both lack support for robust mobility, i.e. there is no second chance of an HO trigger or HO signalling.

Fig. 14 shows the results of the average RLF rate. Dual-link HO exhibited no RLFs because there is always a second chance of an HO trigger. That is, an HOF can only occur after the first HO operation begins. PHO exhibited the highest RLF HO failure as it cannot prevent RLFs before the completion of a micro-macro HO procedure.

Fig. 15 shows the results of the average PP rate. The average PP rate of CU-split HO was the least because it must satisfy two HO conditions for an inter-macro eNB HO procedure, which includes both the macro-macro HO and the micro-micro HO. The average PP rate in all of the HO schemes can be reduced by either increasing H or T_{TTT} in common.

Fig. 16 shows the results of the average service interrupt time. The service interrupt time refers to the time for the C-plane transition and does not include the cases of RLF or HOF. The average service interrupt time of PHO was the least as its C-plane transitions between macro eNBs use the X2 interface, not the radio.

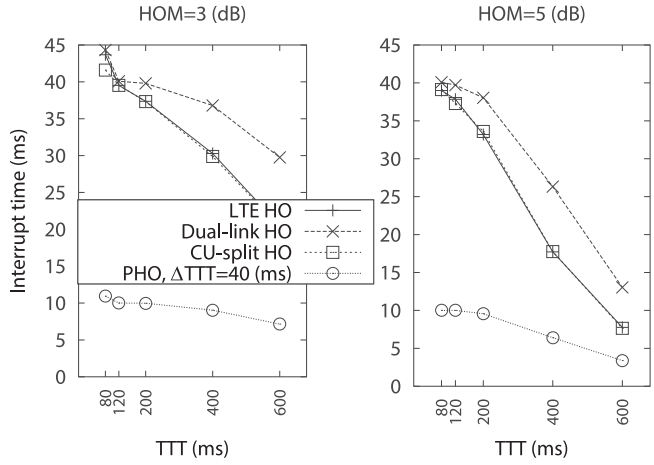

Fig. 16. Performance comparison of average service interrupt time among LTE-A HO, Dual-link HO, CU-split HO, and PHO schemes.

TABLE III
COMPARISON OF HO SIGNALLING

	No. of LTE-Uu signalling	No. of X2 signalling	No. of S1 signalling	No. of total signalling	Total duration (ms)
Micro-macro HO	6	6	2	14	90
Macro-micro HO	12	10	2	24	100
PHO	18	16	4	36	190
LTE-A HO	6	4	2	12	90

VII. DISCUSSION

According to the results of the above performance evaluation, under certain configurations, PHO achieved not only an average successful handover rate approaching 100% but also approximately 10 ms of average service interrupt time less than that of Dual-link HO. Thus, we summarize the following causes and effects:

1) Improving mobility robustness using diversity gain (e.g., transmit and time diversities) can achieve a reduced HOF rate. The cost of this improvement is the requirement of additional signalling overhead. For example, we offer the HO signalling comparison between PHO and LTE-A HO in Table III, where the count of the PHO signalling corresponds with the signalling indicated in the message flow diagrams in Figs. 5 and 8. In the PHO, approximately triple the total amount of HO signalling is required as both the micro-macro and macro-micro HO procedures must be performed. By exploiting the C-plane transition through an X2 interface, the total duration of the macro-micro HO consists of the periods T_{MRS} and T_{CoS}, which are modeled as 10 ms and 90 ms respectively. Thus, approximately twice the total HO duration of PHO is required compared to that of LTE-A HO.
2) An a priori method (e.g., a method of two-level HO triggering, two-level HO triggering, or HO prefetching) can achieve shorter average service interrupt time by completing context exchange or future operation in advance

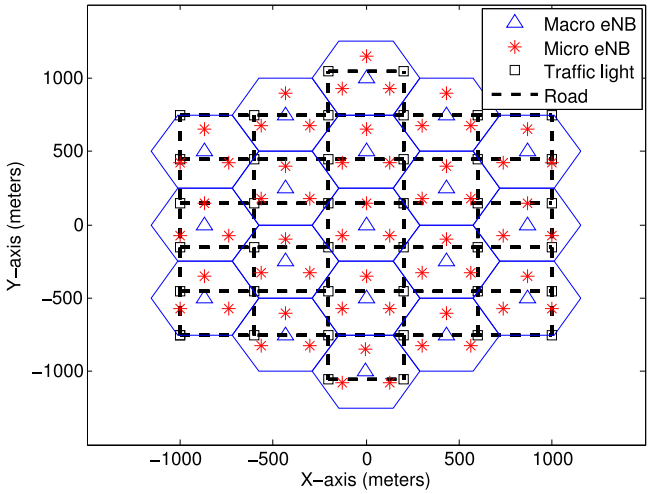

Fig. 17. Urban layout with the mobility model of Simulation of Urban MObility (SUMO).

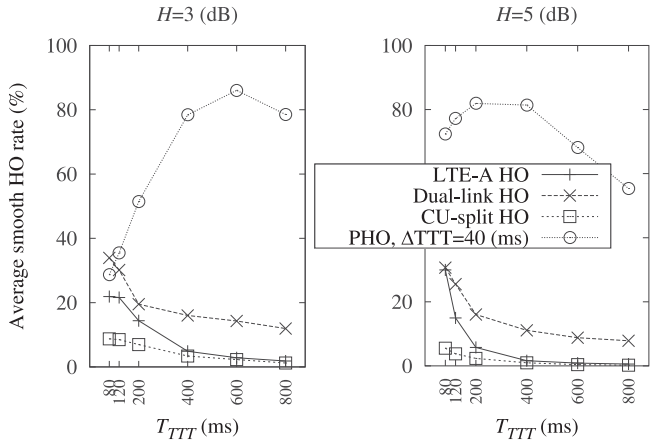

Fig. 18. Performance comparison of average smooth HO rate among LTE-A HO, Dual-link HO, CU-split HO, and PHO schemes for the urban scenario.

of their requirement. This improvement costs additional eNB resources (e.g., CPU loading and memory usage) as the resources are required for the C-plane transition. If a mismatch between the final eNB and the target eNB occurs, the HO triggering of the a priori method is ineffective.

3) A HO condition must be sufficiently stringent (e.g., reducing the length of TTT timer or decreasing the HO threshold) to ensure that the PP rate is satisfactorily reduced. If an HO condition is overly stringent, it increases the HOF rate.

Furthermore, RLFs, which occur on the MR side, are inevitable when an HO process has not yet been started. They are difficult to address using mobility improvement. Possible methods are related to L1 optimization frameworks (e.g., power control and interference cancellation) associated with detection-based or prediction-based algorithms.

In addition, to observe the performance of PHO under a different environment with realistic mobility, we used Simulation of Urban MObility (SUMO) [32] to simulate the two-dimensional network layout in an urban setting (including intersections and traffic lights), which is shown in Fig. 17. We repeated multiple independent experiments for the simulation results. In each experiment, MRs were randomly distributed on roads and routed with a speed range by SUMO. This simulation settings also follow the simulation guidelines recommended by 3GPP [33], [34]. The MR speed ranged between 0 km/h and 54 km/h and the simulation time was 100 seconds. Fig. 18 displays the performance of the average smooth HO rate, which is defined as the ratio that an MR can finish its route without any failure or PP effect during the simulation time. PHO significantly outperformed the others with Dual-Link HO as the second best. This is because Dual-Link HO lacks any prediction method for a dynamic route whereas PHO uses the micro-macro HO procedure to predict and preconnect a target macro eNB. Moreover, to maintain the certain mobility robustness for PHO, the macro-micro HO can fall back to the LTE-A HO in the event of a prediction error. Therefore, the prediction method facilitates mainly accurate prefetching. LTE-A HO and CU-split HO finished in the third and fourth places because they lack any mobility improvement and, for CU-split HO, the inefficient combination of the C/U-plane-split architecture and inter-macro eNB HO caused its procedure to be triggered in an untimely manner.

VIII. Conclusion

In a C/U-plane-split network for a high-speed railway communication system, the inter-macro eNB HO is similar to the LTE-A HO. The results of the averages of both successful HO rate and service interrupt time indicated that they were unreliable and inefficient. Considering the causes of HOFs, which are related to both the RLM and HO processes according to the LTE-A specification, we proposed a DC-based prevenient HO scheme to improve robustness. We integrated the operations of the LTE-A DC technique into the proposed scheme. Further, we presented the designs in detail for the feasibility and computability with the current 4G LTE-A system. There are two key concepts. First, HOFs are caused by the poor reception of RRC HO signalling; hence, the RRC HO signalling duplication of the proposed scheme is effective during the HO procedure. Moreover, after the micro-macro HO procedure of the proposed scheme, the target macro eNB becomes the SeNB to a MR in advance. As the bearers between the MR and the target macro eNB are previously prepared, the master-secondary role switch for the C-plane transition completes quickly. In summary, more preparations for both radio access and C-plane transition reduce the time of their execution. Furthermore, we developed the analytical expressions for the successful HO trigger probabilities, where the effect of an RLF on an HO procedure was considered, for the proposed scheme and the LTE-A HO. The analytical results were verified against simulation results. Through performance evaluations of PHO, LTE-A, CU-split, and Dual-link HOs, we summarized the causes, effects, and costs of the HOs, which should be helpful to future HO research.

References

[1] "Evolved Universal Terrestrial Radio Access (E-UTRA) and Evolved Universal Terrestrial Radio Access Network (E-UTRAN); Overall description, Stage2," 3GPP TS 36.300 version 14.0.0, Sep. 2016.

[2] "Evolved Universal Terrestrial Radio Access (E-UTRA); Study on mobile relay," 3GPP TR 36.836 version 12.0.0, Jun. 2014.
[3] M. Pan *et al.*, "An enhanced handover scheme for mobile relays in LTE-A high-speed rail networks," *IEEE Trans. Veh. Technol.*, vol. 64, no. 2, pp. 743–756, Feb. 2015.
[4] "Study on small cell enhancements for E-UTRA and E-UTRAN; higher layer aspects," 3GPP TR 36.842 version 12.0.0, Dec. 2013.
[5] "Requirements, Candidate Solution and Technology Roadmap for LTE Rel-12 onward," 3GPP RWS-120010, Jun. 2012.
[6] H. Ishii *et al.*, "A novel architecture for LTE-B: C-plane/U-plane split and phantom cell concept," in *Proc. IEEE Globecom Workshops*, Dec. 2012, pp. 624–630.
[7] "Study on control and user plane separation of EPC nodes," 3GPP TR 23.714 version 14.0.0, Jun. 2016.
[8] M. Joud *et al.*, "Selective C-/U-plane split and CoMP to improve moderate speed users performance in small cell deployments," in *Proc. IEEE Int. Conf. Wireless Mobile Comput., Netw. Commun.*, Oct. 2014, pp. 697–702.
[9] N. Meng *et al.*, "Virtual cell-based mobility enhancement and performance evaluation in ultra-dense networks," in *Proc. Wireless Commun. Netw. Conf.*, Apr. 2016, pp. 1–6.
[10] H. Song *et al.*, "Handover scheme for 5G C/U plane split heterogeneous network in high-speed railway," *IEEE Trans. Veh. Technol.*, vol. 63, no. 9, pp. 4633–4646, Apr. 2014.
[11] L. Gimenez *et al.*, "Analysis of data interruption in an LTE highway scenario with dual connectivity," in *Proc. IEEE Veh. Technol. Conf. Spring*, May 2016, pp. 1–5.
[12] C. Rosa *et al.*, "Dual connectivity for LTE small cell evolution: Functionality and performance aspects," *IEEE Commun. Mag.*, vol. 54, no. 6, pp. 137–143, Jun. 2016.
[13] M. Polese *et al.*, "Improved handover through dual connectivity in 5G mmWave mobile networks," *IEEE J. Sel. Areas Commun.*, vol. 35, no. 9, pp. 2069–2084, Sep. 2017.
[14] M. Polese *et al.*, "Performance comparison of dual connectivity and hard handover for LTE-5G tight integration," in *Proc. EAI Int. Conf. Simul. Tools Techn.*, Aug. 2016, pp. 118–123.
[15] L. Tian *et al.*, "Seamless dual-link handover scheme in broadband wireless communication systems for high-speed rail," *IEEE J. Sel. Areas Commun.*, vol. 30, no. 4, pp. 708–718, May 2012.
[16] T. Guo *et al.*, "Seamless handover for LTE macro-femto networks based on reactive data bicasting," *IEEE Commun. Lett.*, vol. 16, no. 11, pp. 1788–1791, Nov. 2012.
[17] Y. Xia *et al.*, "Coordinated of multi-point and bi-casting joint soft handover scheme for high-speed rail," *IET Commun.*, vol. 8, no. 14, pp. 2509–2515, Sep. 2014.
[18] M. Chuang and M. Chen, "NASH: Navigation-assisted seamless handover scheme for LTE-A smallcell networks," in *Proc. IEEE Int. Conf. Commun.*, Jun. 2015, pp. 3952–3957.
[19] X. Yu *et al.*, "An optimized seamless dual-link handover scheme for high-speed rail," *IEEE Trans. Veh. Technol.*, vol. 65, no. 10, pp. 8658–8668, Oct. 2016.
[20] S. Xie *et al.*, "A seamless dual-link handover scheme with optimized threshold for C/U plane network in high-speed rail," in *Proc. IEEE Veh. Technol. Conf. Spring*, May 2016, pp. 1–5.
[21] "Evolved Universal Terrestrial Radio Access (E-UTRA); mobility enhancements in heterogeneous networks," 3GPP TR 36.839 version 0.7.1, Aug. 2012.
[22] K. Kanwal and G. Safdar, "Reduced early handover for energy saving in LTE networks," *IEEE Commun. Lett.*, vol. 20, no. 1, pp. 153–156, Dec. 2015.
[23] G. Kollias *et al.*, "Handover performance in LTE-A HetNets through inter-site distance differentiation," in *Proc. IEEE Int. Workshop Comput. Aided Modeling Design Commun. Links Netw.*, Dec. 2014, pp. 280–284.
[24] J. Puttonen *et al.*, "Radio problem detection assisted rescue handover for LTE," in *Proc. IEEE Int. Symp. Personal Indoor Mobile Radio Commun.*, Dec. 2010, pp. 1752–1757.
[25] K. Dimou *et al.*, "Handover within 3GPP LTE: Design principles and performance," in *Proc. IEEE Veh. Technol. Conf. Fall*, Sep. 2009, pp. 1–5.
[26] M. Anas *et al.*, "Performance analysis of handover measurements and layer 3 filtering for utran LTE," in *Proc. IEEE Int. Symp. Personal Indoor Mobile Radio Commun.*, Sep. 2007, pp. 1–5.
[27] C. Lima *et al.*, "Modeling and analysis of handover failure probability in small cell networks," in *Proc. IEEE Conf. Comput. Commun. Workshops*, Jul. 2014, pp. 736–741.
[28] K. Vasudeva *et al.*, "Analysis of handover failures in HetNets with layer-3 filtering," in *Proc. Wireless Commun. Netw. Conf.*, Apr. 2014, pp. 2647–2652.
[29] D. Lpez-Prez *et al.*, "Theoretical analysis of handover failure and ping-pong rates for heterogeneous networks," in *Proc. IEEE Int. Conf. Commun.*, Jun. 2012, pp. 6774–6779.
[30] "NR and NG-RAN Overall Description; Stage 2," 3GPP TS 38.300 version 1.0.0: NR, Sep. 2017.
[31] "WINNER II Channel Models: Part I Channel Models," IST-4-027756 WINNER II D1.1.2 V1.2, Feb. 2008.
[32] SUMO, [Online]. Available: "http://www.gctsemi.com/"
[33] "Evolved Universal Terrestrial Radio Access (E-UTRA); Further advancements for E-UTRA physical layer aspects," 3GPP TR 36.814 version 9.2.0, Mar. 2017.
[34] "Study on LTE-based V2X services," 3GPP TR 36.855 version 14.0.0, Jun. 2016.

Ping-Jung Hsieh received the B.S. degree in computer science and information engineering from Chang Gung University, Taoyuan, Taiwan, in 2009. He received the M.S. degree in communication engineering from National Central University, Taoyuan, in 2011. He received the Ph.D. degree in electrical engineering from National Taiwan University, Taipei, Taiwan, in 2017. His research interests include mobile networking, broadband wireless access networks, and advanced system architecture aspects. He has 5G/4G testbed development experience in system/protocol design, evaluation, and implementation.

Wei-Shih Lin received the B.S. degree in electrical and computer engineering from National Chiao Tung University, Taoyuan, Taiwan, in 2013. He received the M.S. degree in communication engineering from National Taiwan University, Taipei, Taiwan, in 2016. His research interests include Mobile Communications Design for 5G wireless communication systems.

Kuang-Hsun Lin received the B.S. degree in electrical engineering degree from National Taiwan University, Taipei, Taiwan, in 2015. He is currently working toward the Ph.D. degree in communication engineering at National Taiwan University, GICE, Taipei. Since 2015, he has been working with Wireless Mobile Networking Laboratory led by Professor H.Y. Wei. He held summer internships at Mediatek in summer 2015.

Hung-Yu Wei received the B.S. degree in electrical engineering from National Taiwan University (NTU), Taipei, Taiwan. He received the M.S. and Ph.D. degrees in electrical engineering from Columbia University, New York, NY, USA. He was a summer intern at Telcordia Applied Research in 2000 and 2001. He was with NEC Labs America from 2003 to 2005. He joined NTU in 2005. He is currently a Professor with the Department of Electrical Engineering and Graduate Institute of Communication Engineering at NTU. His research interests include broadband wireless, vehicular networking, IoT, and game theoretic models for networking. He actively participates in wireless communications standardization activities. He was the recipient of the K. T. Li Young Researcher Award from ACM Taipei Chapter and IICM in 2012, CIEE Excellent Young Engineer Award in 2014, and the NTU Excellent Teaching Award in 2008. He also received the Wu Ta You Memorial Award from the Ministry of Science and Technology in 2015. He is currently the Chair of the IEEE VTS Taipei Chapter.